

HEAT AND MASS TRANSFER AT CHEMICAL TRANSFORMATIONS

MATHEMATICAL MODELING OF THE INITIATION AND SPREAD OF PEAT FIRES

A. M. Grishin and A. S. Yakimov

UDC 511.534.536.245.022

We propose a new statement and a numerical solution of the problem on ignition of a peat bed as a result of the action of the nucleation site of a low fire on the basis of the mathematical model of a porous reactive medium. It has been obtained that at moderate temperatures ($T_2 \leq 750$ K) the smoldering of the original reactant is determined by the processes of heat and mass exchange with the nucleation site of the forest fire, drying, and pyrolysis of peat, as well as by the oxidation reaction of carbon oxide, the peat height, and the thickness of the water stratum under its bed.

Keywords: peat, drying, pyrolysis, smoldering, water.

Introduction. In [1], on the basis of observational results for peat fires in the Tomsk region a general mathematical model of forest fires was proposed. The results of experimental investigations of peat fires were published in [2–4]. Subsequently, on the basis of [1], we carried out a series of works at mathematical modeling of peat fires [5, 6] that confirmed the physical fundamentals of the mathematical model of [1]. In [7], we proposed a refined mathematical model of peat fires of the second generation that takes into account the two-temperature character of a porous medium, the particles of ash, soot, smoke, and free water, and the influence of the multicomponent character of the gas medium. In [8], a review of the investigations of peat fires is given. In [9], we investigated the process of peat ignition in the one-dimensional, one-temperature statement, and in [10] we modeled the moldering of peat over a water layer in the two-temperature, axisymmetric statement.

In the present work, on the basis of the models of [1, 7] with account for the experimental data of [11, 12], we investigate the initiation of an underground fire when a three-dimensional peat bed (Fig. 1) situated over a water layer ignites on the top, and the combustion front propagates into the stratum under different external conditions and initial moisture contents of peat.

1. Formulation of the Problem. Let us assume that a peat bog fire breaks out as a result of ignition from a surface place of combustion whose action on the peat bed is modeled by the temperature of the place of combustion T_c and the heat and mass transfer coefficients α_c and β_c . We consider the spatial problem in a parallelepiped (Fig. 1) where the x_3 axis is directed vertically down and the origin of coordinates on the x_3 axis is chosen at the interface between the peat bed and the atmosphere. It is assumed that peat is a two-dimensional medium, i.e., the gas phase and the condensed phase (framework) have different temperatures.

It is thought that under the stratum of the porous medium there is a water layer having a temperature differing from the peat temperature. We assume that at the peat-water interface the peat temperature is lower than the boiling temperature of water and the heat transfer at the peat bed–water layer interface can be neglected. On the basis of the analysis of the experimental data presented in [2, 11, 12] and theoretical investigations [1, 7] we assume that peat ignition leads to the formation of a combustion front consisting of peat heating, drying, and pyrolysis zones, as well as of zones of combustion of gaseous and condensed products of pyrolysis followed by the formation of an ash layer.

In accordance with the results of [1, 7] it is assumed that in the peat bed itself there occur bound water evaporation, an exothermal reaction of coke breeze combustion, as well as homogeneous reactions of peat pyrolysis and combustion of carbon oxide and methane. Peat in the process of ignition was regarded as a multiphase medium

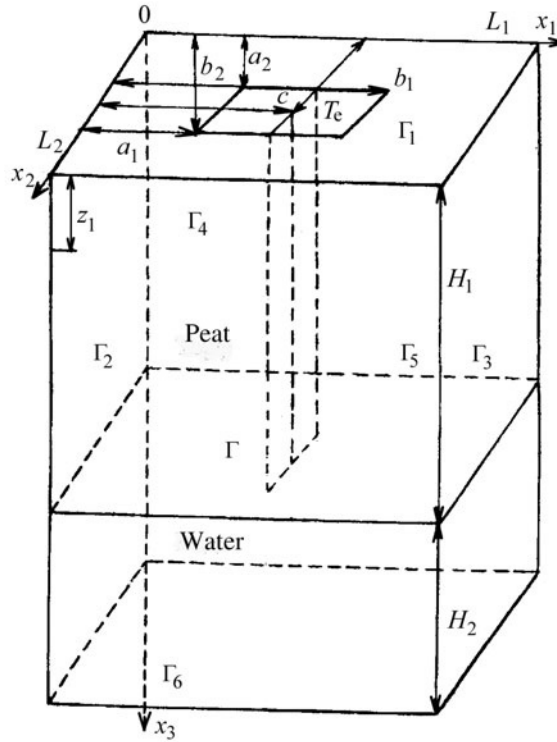


Fig. 1. Scheme of the heat exchange of peat on the water stratum with the environment.

consisting of a dry organic substance with a volume fraction φ_1 , hygroscopic water with a volume fraction φ_2 bound to this organic substance [7], a pyrolysis product of the organic substance (coke breeze with a volume fraction φ_3), as well as condensed and gaseous combustion products (volume fractions φ_4 and φ_5). It was assumed that the gas phase in the peat bed consists of six components: CO, H₂O, O₂, CO₂, CH₄, and N₂ with mass concentrations c_α , where $\alpha = 1 - 6$, respectively. Since the influence of the heat release from the combustion of the hydrogen component H₂ is not strong by virtue of its insignificant initial concentration and the relatively low temperatures noted in the process of smoldering of the permeable peat bed, the H₂ concentration was not taken into account. We considered such a peat bed in which the initial volume fraction of the gas phase φ_{5in} ($0.05 < \varphi_{5in} < 0.2$) is small compared to the volume fractions of the condensed phase. This mathematical model presents a particular case of the model proposed in [7]. It is known that in the process of peat bed combustion, as a result of pyrolysis, coke is formed [1, 7] and then smolders in the course of the exothermal oxidation reaction. In general, it is assumed that the front of the peat fire, when deep in the peat bed, consists of heating, drying, pyrolysis, and combustion zones of the gaseous and condensed products of pyrolysis of dried peat and an ash layer.

The above mathematically formulated problem with account for the assumptions made is reduced to the solution of the following system of equations [1, 7]:

$$\frac{\partial \rho_5 \varphi_5}{\partial t} + \text{div} (\rho_5 \varphi_5 \mathbf{W}) = Q, \quad (1)$$

$$\text{grad } P = -\frac{\mu}{\xi} \mathbf{W}, \quad (2)$$

$$\sum_{i=1}^4 c_{is} \rho_{is} \varphi_i \frac{\partial T_1}{\partial t} = \text{div} (\lambda_s \text{grad } T_1) + A_v (T_2 - T_1) + \sum_{i=1}^4 q_{is} R_{is}, \quad (3)$$

$$\begin{aligned} \rho_5 \varphi_5 c_{p5} \frac{dT_2}{dt} &= \operatorname{div} (\lambda_5 \varphi_5 \operatorname{grad} T_2) + \rho_5 \varphi_5 \operatorname{grad} T_2 \sum_{\alpha=1}^N c_{p\alpha} D_\alpha \operatorname{grad} c_\alpha \\ &+ A_v (T_1 - T_2) + c_{1s} (T_1 - T_2) (1 - \alpha_c) R_{1s} + c_{2s} (T_1 - T_2) R_{2s} + q_1 r_1 + q_2 r_2, \end{aligned} \quad (4)$$

$$\rho c_p \frac{\partial T}{\partial t} = \operatorname{div} (\lambda \operatorname{grad} T), \quad (5)$$

$$\rho_5 \varphi_5 \frac{dc_\alpha}{dt} = \operatorname{div} (\rho_5 \varphi_5 D_\alpha \operatorname{grad} c_\alpha) - c_\alpha Q + R_\alpha, \quad \alpha = 1, \dots, N-1, \quad (6)$$

$$\rho_{1s} \frac{\partial \varphi_1}{\partial t} = -R_{1s}, \quad \rho_{2s} \frac{\partial \varphi_2}{\partial t} = -R_{2s}, \quad \rho_{3s} \frac{\partial \varphi_3}{\partial t} = \alpha_c R_{1s} - R_{3s} - \alpha_4 R_{3s}, \quad \rho_{4s} \frac{\partial \varphi_4}{\partial t} = R_{4s}, \quad (7)$$

$$\sum_{\alpha=1}^N c_\alpha = 1, \quad \varphi_5 = 1 - \sum_{i=1}^4 \varphi_i, \quad M^{-1} = \sum_{\alpha=1}^N \frac{c_\alpha}{M_\alpha}, \quad P = \frac{\rho_5 R T_2}{M}. \quad (8)$$

To solve the system of equations (1)–(7), we used the following initial and boundary conditions:

$$\begin{aligned} T_i |_{t=0} &= T |_{t=0} = T_{\text{in}}, \quad i = 1, 2, \quad c_\alpha |_{t=0} = c_{\alpha \text{in}}, \quad \alpha = 1, 2, \dots, N-1, \\ \rho_5 |_{t=0} &= \rho_{5 \text{in}}, \quad \varphi_i |_{t=0} = \varphi_{i \text{in}}, \quad i = 1, \dots, 4; \end{aligned} \quad (9)$$

the balance boundary conditions [13]

$$\begin{aligned} (1 - \varphi_5) \alpha_e (T_e - T_{1, \Gamma_1}) &= \lambda_s \left. \frac{\partial T_1}{\partial x_3} \right|_{\Gamma_1}, \quad a_i \leq x_i \leq b_i, \quad i = 1, 2, \quad x_3 = 0, \\ (1 - \varphi_5) \alpha_{a_i} (T_e - T_{1, \Gamma_1}) &= \lambda_s \left. \frac{\partial T_1}{\partial x_3} \right|_{\Gamma_1}, \quad 0 \leq x_i < a_i, \quad b_i < x_i \leq L_i, \quad i = 1, 2, \quad x_3 = 0, \\ \varphi_5 \alpha_e (T_e - T_{2, \Gamma_1}) &= \lambda_5 \varphi_5 \left. \frac{\partial T_2}{\partial x_3} \right|_{\Gamma_1}, \quad a_i \leq x_i \leq b_i, \quad i = 1, 2, \quad x_3 = 0, \\ \varphi_5 \alpha_{a_i} (T_e - T_{2, \Gamma_1}) &= \lambda_5 \varphi_5 \left. \frac{\partial T_2}{\partial x_3} \right|_{\Gamma_1}, \quad 0 \leq x_i < a_i, \quad b_i < x_i \leq L_i, \quad i = 1, 2, \quad x_3 = 0; \end{aligned} \quad (10)$$

the conjugation conditions at the peat–water interface [9, 10]

$$\lambda_s \left. \frac{\partial T_1}{\partial x_3} \right|_{\Gamma_-} = \lambda \left. \frac{\partial T}{\partial x_3} \right|_{\Gamma_+} - \frac{q_{2s} R_{2s}}{s_2}, \quad T_1 |_{\Gamma_-} = T |_{\Gamma_+} = T_2 |_{\Gamma_-}, \quad 0 \leq x_i \leq L_i, \quad i = 1, 2, \quad x_3 = H_1; \quad (11)$$

on the faces Γ_m ($m = 2 - 5$) we give the heat transfer by the Newton law at $0 < x_3 < H_1$

$$\lambda_s \frac{\partial T_1}{\partial x_1} \Big|_{\Gamma_m} = \alpha_{\Gamma_m} (T_{1,\Gamma_m} - T_{\text{in}}), \quad \lambda_5 \varphi_5 \frac{\partial T_2}{\partial x_1} \Big|_{\Gamma_m} = \alpha_{\Gamma_m} (T_{2,\Gamma_m} - T_{\text{in}}), \quad m=2, 3,$$

$$0 \leq x_i \leq L_i, \quad i=2, 3, \quad \alpha_{\Gamma_m} = \alpha_{\text{in}} (1 - 0.9x_3), \quad m=2-5, \quad L_3 = H_1 + H_2,$$

$$\lambda_5 \varphi_5 \frac{\partial T_2}{\partial x_2} \Big|_{\Gamma_m} = \alpha_{\Gamma_m} (T_{2,\Gamma_m} - T_{\text{in}}), \quad m=4, 5, \quad 0 \leq x_i \leq L_i, \quad i=1, 3,$$

and the heat insulation condition at $H_1 < x_3 < L_3$

$$\frac{\partial T}{\partial x_i} \Big|_{\Gamma_m} = 0, \quad i=1, 2, \quad m=2-5, \quad H_1 < x_3 < H_1 + H_2,$$

(12)

$$T \Big|_{\Gamma_6} = T_{\text{in}}, \quad 0 \leq x_i \leq L_i, \quad i=1, 2, \quad x_3 = H_1 + H_2.$$

Using the analogy of the heat and mass transfer processes [14] ($\beta_e = \alpha_e / c_{p5}$), we have the boundary conditions

$$\beta_e (c_{\alpha,e} - c_{\alpha,w}) = \varphi_5 \rho_5 D_\alpha \frac{\partial c_\alpha}{\partial x_3} \Big|_{\Gamma_1}, \quad a_i \leq x_i \leq b_i, \quad i=1, 2, \quad x_3 = 0,$$

$$\beta_{L_i} (c_{\alpha,a_i} - c_{\alpha,w}) = \varphi_5 \rho_5 D_\alpha \frac{\partial c_\alpha}{\partial x_3} \Big|_{\Gamma_1}, \quad 0 \leq x_i < a_i, \quad b_i < x_i \leq L_i, \quad i=1, 2, \quad x_3 = 0,$$

(13)

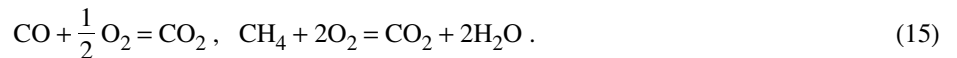
$$\beta_{\Gamma_m} (c_{\alpha,\text{in}} - c_{\alpha,\Gamma_m}) = \varphi_5 \rho_5 D_\alpha \frac{\partial c_\alpha}{\partial x_1} \Big|_{\Gamma_m}, \quad m=2, 3, \quad 0 \leq x_2 \leq L_2, \quad 0 < x_3 < H_1,$$

$$\beta_{\Gamma_m} (c_{\alpha,\text{in}} - c_{\alpha,\Gamma_m}) = \varphi_5 \rho_5 D_\alpha \frac{\partial c_\alpha}{\partial x_2} \Big|_{\Gamma_m}, \quad m=4, 5, \quad 0 \leq x_1 \leq L_1, \quad 0 < x_3 < H_1,$$

$$P \Big|_{\Gamma_1} = P_e, \quad \frac{\partial c_\alpha}{\partial x_3} \Big|_{\Gamma} = 0, \quad \frac{\partial P}{\partial x_3} \Big|_{\Gamma} = 0, \quad \frac{\partial P}{\partial x_i} \Big|_{\Gamma_m} = 0, \quad i=1, 2, \quad m=2-5.$$

(14)

2. Transfer Coefficients, Thermophysical and Thermokinetic Constants. The final homogeneous chemical reactions in the permeable peat bed [1, 15] are given as



(15)

The chemical kinetics equations for the carbon oxide and methane oxidation reactions have the form [16]

$$\frac{dy_1}{dt} = -k_1 x_1 x_3^{0.25} T_2^{-2.25} \exp\left(-\frac{E_1}{RT_2}\right) = r_1, \quad \frac{dy_2}{dt} = -k_2 x_5^{-0.5} x_3^{1.5} \frac{P}{T_2} \exp\left(-\frac{E_2}{RT_2}\right) = r_2.$$

For bound water evaporation in the multiphase medium — peat — the analog of the Hertz–Knudsen law [1, 15]

$$R_{2s} = \frac{s_2 M_2 A_s \Phi_2 [k_{2s} \exp(-E_{2s}/RT_1) - P_2]}{(2\pi RT_1 M_2)^{0.5}} \quad (16)$$

is used. To find the partial pressure of water vapors in the peat bed P_2 , we use the Dalton law [1, 15] according to which $P_2/P = x_2$. Then for P_2 we have the expression

$$P_2 = P c_2 \frac{M}{M_2}.$$

The effective diffusion coefficient is obtained by the Fristrom–Westenberg formula [14, 17]:

$$D_\alpha = (1 - c_\alpha) \left(\sum_{\substack{j=1 \\ j \neq \alpha}}^N \frac{x_j}{d_{\alpha,j}} \right)^{-1}, \quad d_{\alpha,j} = 1.66 \cdot 10^{-7} \frac{[(M_\alpha + M_j)/(M_\alpha M_j)]^{0.5} T_2^{1.67}}{P \sigma_{j,\alpha}^2 (\epsilon_{j,\alpha}/kT_2)^{0.17}}.$$

The formula for the heat conductivity coefficients of the gas phase component λ_j , $j = 1, 2, \dots, N$ was taken from [18]

$$\lambda_5 = \sum_{i=1}^N \lambda_i c_i, \quad \lambda_j = \lambda_j^0 \left(0.115 + 0.354 \frac{c_{pj}}{R} \right), \quad \lambda_i^0 = 8.32 \cdot 10^{-2} \frac{M_i^{-0.5} T_2^{0.647}}{\sigma_i^2 (\epsilon_i/kT_2)^{0.147}},$$

$$c_{p5} = \sum_{j=1}^N c_{pj} c_j, \quad \lambda_s = \sum_{i=1}^4 \lambda_{is} \Phi_i.$$

The heat capacity coefficients of the gas phase component $c_{pj} = a_j + b_j T_2 + c_j/T_2^2$ were taken from [19], and the values of the quantities λ_{is} in the condensed phase are given in [1, 14].

The expressions for $R_1 - R_5$, Q , $R_{1s} - R_{4s}$, α_c , $\eta_1 - \eta_4$ in Eqs. (1), (3), (4), (6), (7) have the form [9, 10]

$$R_1 = \eta_1 R_{1s} - M_1 r_1, \quad R_2 = \eta_2 R_{1s} - R_{2s} + 2M_2 r_2, \quad R_3 = -\eta_3 R_{3s} - M_3 r_1/2 - 2M_3 r_2, \quad R_4 = M_4 (r_1 + r_2), \quad R_5 = \eta_4 R_{1s} - M_5 r_2, \quad R_{1s} = k_{1s} \rho_{1s} \Phi_1 \exp\left(-\frac{E_{1s}}{RT_1}\right),$$

$$R_{3s} = \frac{M_c}{M_3} s_3 k_{3s} \Phi_5 \rho_5 \Phi_3 c_3 \exp\left(-\frac{E_{3s}}{RT_1}\right), \quad Q = (1 - \alpha_c) R_{1s} + R_{2s} + R_{3s},$$

$$R_{4s} = \alpha_4 R_{3s}, \quad \alpha_c = \frac{M_c}{M_{in} - M_c}, \quad \eta_1 = \frac{M_1}{M_{in}}, \quad \eta_2 = \frac{M_2}{M_{in}}, \quad \eta_3 = \frac{M_3}{M_{in}}, \quad \eta_4 = \frac{M_4}{M_{in}}.$$

3. Computational Procedure and Input Data. The system of equations (1)–(7) with the boundary conditions (9)–(14) was solved by the iteration-interpolation method [20]. For the variant $\Phi_{1in} = 0.7$, $\Phi_{2in} = 0.2$, $c_{3in} = 0.23$, T_e

$= 1100$ K, $\alpha_c = 1.5$ W/(K·m²), $\sum_{i=1}^4 \rho_{is} \Phi_{iin} = 925$ kg/m³, $\rho_{1s} = 750$ kg/m³ and the input data from this section, we carried out the procedure of testing the numerical method. To solve the mathematical model, we used a sequence of space thickening meshes: $h_{x_3} = 2.5 \cdot 10^{-3}$ m, $h_{x_2} = 10^{-2}$ m, $h_{x_1} = 10^{-2}$ m and took $h_i = 2h_{x_i}$, $h_i = h_{x_i}/2$, $h_i = h_{x_i}/4$, $h_i = h_{x_i}/8$, $i = 1, 2, 3$.

TABLE 1. Influence of the Condensed Phase Density, the Heat Transfer Coefficient, and the Ambient Temperature on the Ignition Time of Peat Samples

ρ_{1s} , kg/m ³	Φ_{1in}	Φ_{2in}	α_e , W/(K·m ²)	T_e , K		
				1200	1100	1000
<i>Ignition time of peat samples</i>						
1200	0.7	0.05	1.5	5.9	6.48	7.45
			1.25	6.4	7.1	8.8
			1.0	8.5	9.98	—
1000	0.7	0.1	1.5	6.1	7.96	8.78
			1.25	7.85	8.94	12.86
			1.0	10.6	14.76	—
750	0.7	0.2	1.75	5.07	6.81	9.67
			1.5	6.92	10.83	14.17
			1.25	10.47	14.83	—
			1.0	18.36	—	—

The following parameters were registered: the ignition time t_* of the peat–water system when the peat (gas) surface temperature T_{2w} reaches 750 K, the temperature value of the peat (framework, gas) on the surface and in the depth at various instants of time, as well as the mean value of the smoldering rate of peat depending on the time. In so doing, the time step was variable and was generated automatically according to the given accuracy equal for all meshes in the space.

The ignition time t_* error decreased: $\varepsilon_1 = 16\%$, $\varepsilon_2 = 8.2\%$, $\varepsilon_3 = 3.7\%$. The tendency for a decrease in the error for the peat (framework, gas) temperature is preserved: $\varepsilon_1 = 7.2\%$, $\varepsilon_2 = 2.4\%$, $\varepsilon_3 = 1.1\%$. The discrepancy between the results on the means smoldering rate also decreases: $\varepsilon_1 = 19\%$, $\varepsilon_2 = 10.1\%$, $\varepsilon_3 = 5.2\%$.

The linear rate of smoldering of the peat surface was determined by the formula

$$\omega_3 = \frac{(\Delta x_3)_*}{(\Delta t)_*} = \frac{x_3(k) - x_3(k-1)}{t_*(k) - t_*(k-1)}, \quad \omega_1 = \frac{(\Delta x_1)_*}{(\Delta t)_*} = \frac{x_1(j) - x_1(j-1)}{t_*(j) - t_*(j-1)}. \quad (18)$$

In (18), $t_*(k)$ and $t_*(k-1)$ denote the time of reaching the smoldering temperature T_* at $x_3 = x_3(k)$ and $x_3 = x_3(k-1)$, where k is the current bed and $(k-1)$ — the previous bed on the x_3 axis, with $\omega_3 = \omega_3(x_1 = x_2 = c)$ and $\omega_1 = \omega_1(x_2 = c, x_3 = 0)$. The values of $t_*(j)$ and $t_*(j-1)$ on the x_1 axis are determined in much the same manner. For the thermophysical and thermokinetic parameters of peat, the data of [1–3, 9, 14, 15, 21] were used. The thermophysical characteristics of water and water vapor were taken from [22]. The results given below were obtained at $T_{in} = 293$ K, $T_* = 650$ K, $\omega_* = 5 \cdot 10^{-6}$ m/s, $P_e = P_{in} = 1.013 \cdot 10^5$ N/m², $T_e = 1000$ – 1200 K, $\mu_{in} = 1.81 \cdot 10^{-5}$ kg/(m·s), $\alpha_{ai} = 1.5$ W/(K·m²), $1.0 \leq \alpha_e \leq 2.0$ W/(K·m²), $A_v = 10^4$ W/(K·m³), $\alpha_{in} = 1.0$ W/(K·m²), $M_1 = 28$ kg/mole, $M_2 = 18$ kg/mole, $M_3 = 32$ kg/mole, $M_4 = 44$ kg/mole, $M_5 = 16$ kg/mole, $M_6 = 28$ kg/mole, $M_c = 12$ kg/mole, $H_1 = 0.5$ m, $H_2 = 0.5$ m, $L_1 = L_2 = 0.5$ m, $\rho_{1s} = 750$ – 1200 kg/m³, $\rho_{2s} = 2 \cdot 10^3$ kg/m³, $\rho_{3s} = 130$ kg/m³, $\rho_{4s} = 130$ kg/m³, $\rho = 10^3$ kg/m³, $c_{1s} = 1.29 \cdot 10^3$ J/(kg·K), $c_{2s} = 2.09 \cdot 10^3$ J/(kg·K), $c_{3s} = 1.02 \cdot 10^3$ J/(kg·K), $c_{4s} = 1.02 \cdot 10^3$ J/(kg·K), $c_p = 4.19 \cdot 10^3$ J/(kg·K), $d_p = 10^{-6}$ m, $R = 8.314$ J/(mole·K), $\lambda_{1s} = 1.67$ W/(m·K), $\lambda_{2s} = 0.6$ W/(m·K), $\lambda_{3s} = 0.041$ W/(m·K), $\lambda_{4s} = 0.041$ W/(m·K), $\lambda = 0.6$ W/(m·K), $A_s = 0.08$, $k_{1s} = 2 \cdot 10^4$ s⁻¹, $E_{1s} = 54.47$ kJ/mole, $q_{1s} = -10^3$ J/kg, $k_{2s} = 10^6$ s⁻¹, $E_{2s} = 16.76$ kJ/mole, $q_{2s} = 1.06 \cdot 10^6$ J/kg, $k_{3s} = 10^5$ m/s, $E_{3s} = 50.28$ kJ/mole, $q_{3s} = 2.81 \cdot 10^5$ J/kg, $q_{4s} = 2.85 \cdot 10^5$ J/kg, $a_1 = a_2 = 0.125$ m, $b_1 = b_2 = 0.375$ m, $c = 0.25$ m, $c_{1in} = 0.1$, $c_{2in} = 5 \cdot 10^{-5}$, $c_{3in} = 0.05$ – 0.23 , $c_{4in} = 10^{-5}$, $c_{5in} = 0.2$, $c_{\alpha,e} = c_{\alpha,in}$, $\alpha = 1, 2, 4, 5$, $c_{3e} = 10^{-3}$, $\Phi_{1in} = 0.6$ – 0.7 , $\Phi_{2in} = 0.05$ – 0.2 , $\Phi_{3in} = 10^{-3}$, $\Phi_{4in} = 10^{-5}$, $s_2 = 0.08$, $s_3 = 0.05$, $\alpha_4 = 0.7$, $\eta_1 = 0.2$, $\eta_2 = 0.02$, $\eta_4 = 0.3$.

4. Results of the Numerical Solution and Their Analysis. We first investigated the regime of ignition and smoldering under various external conditions (ignition from the surface place of combustion). Let us call the time at which a peat fire breaks out the value of $t = t_*$ at which for $T_{2w} \geq T_*$ the smoldering rate ω_3 is equal to the characteristic quantity ω_* or exceeds it, and the surface temperature of the reactant sharply increases to $T_{2w} = 750$ K. For

TABLE 2. Height of the Peat Bed, Thickness of the Water Column, and Heat Transfer Coefficient Depending on the External Place of Combustion and the Reactant Ignition Time

H_2 , m	α_e , W/(K·m ²)	$H_1 = 0.5$ m			$H_1 = 0.25$ m	
		T_e , K				
		1200	1100	1000	1200	1100
<i>Times of different regimes of peat smoldering, t_*, h</i>						
0.5	1.75	5.07	6.81	9.67	8.44	14.44*
	1.5	6.92	10.83	14.17	13.82*	—
	1.25	10.47	14.84	—	—	—
	1.0	18.36	—	—	—	—
0.25	1.75	5.13	6.73	9.75	8.21	14.35*
	1.5	7.01	10.89	14.23	13.69*	—
	1.25	10.53	14.91	—	—	—
	1.0	19.42	—	—	—	—

definiteness, it was assumed that the quantities $T_* = 650$ K and $\omega_* = 5 \cdot 10^{-6}$ m/s were known from the experimental data of [2]. The intermediate regime when the rate of smoldering is an order of magnitude higher than the rate of pyrolysis was observed at $\omega_3 < \omega_*$ in the peat depth. The regime of absence of smoldering of the reactant in which its rate is comparable to the rate of peat pyrolysis arose at $T_{2w} < T_*$. In Tables 1 and 2, the time of the smoldering regime at $\omega_3 < \omega_*$ is marked with an asterisk, and the pyrolysis regime, with a line.

Table 1 presents the ignition time of the reactant at various values of T_e , α_e , ρ_{1s} , φ_{1in} , and φ_{2in} for $c_{3in} = 0.23$, the density values of the condensed phase $\sum_{i=1}^4 \rho_{is} \varphi_{iin} = 925$ kg/m³, and the input data from Section 3. As is seen

from Table 1, with increasing quantity of moisture and decreasing peat density ρ_{1s} (with increasing looseness of the sample) the ignition time increases. This is due to both the excess of the quantity of heat removed by moisture evaporation over the quantity of heat supplied by the exothermal oxidation reaction of carbon oxide and the presence in of air pores that decreases the effective heat conductivity coefficient and increases the heating time of samples. As a result, at 1000 K $\leq T_e \leq 1100$ K, $\alpha_e \leq 1.0$ W/(K·m²), $0.05 \leq \varphi_{2in} \leq 0.2$ ignition does not occur, and the smoldering rates of samples are comparable in the order of magnitude $\omega_3 \sim (1-5) \cdot 10^{-7}$ m/s with the pyrolysis rate of peat. This is due to the decrease in the intensity of action of the external place of combustion and the increase in the quantity of removed heat connected with increase in the quantity of thermal energy expended in water evaporation.

Table 2 presents the ignition time for $\varphi_{1in} = 0.7$, $\varphi_{2in} = 0.2$, $\rho_{1s} = 750$ kg/m³ and other quantities from the data base (see Section 3), but it is absent (the regime of peat pyrolysis) for a different height of the reactant layer, the thickness of the water stratum under it, and the intensity of surface combustion. At a large height of the reactant $H_1 = 0.5$ m (see Table 2) and a thickness of the water column of $0.25 \leq H_2 \leq 0.5$, ignition of peat is observed, except for the variant with a low intensity of external action when $T_e \leq 1100$ K, $\alpha_e \leq 1.0$ W/(K·m²), and $T_e \leq 1000$ K, $\alpha_e \leq 1.25$ W/(K·m²). With decreasing thickness of the peat bed $H_1 = 0.25$ m for $0.25 \leq H_1 \leq 0.5$, reactant smoldering at a rate $\omega_3 < \omega_*$ occurs. With decreasing action of the external place of combustion for $T_e \leq 1100$ K and $\alpha_e \leq 1.75$ W/(K·m²) (see Table 2) peat smoldering does not occur. Finally, at a small thickness of the reactant $H_1 = 0.25$ m the regime of peat smoldering is noted only at a high intensity of external action: $1.5 \leq \alpha_e \leq 1.75$ W/(K·m²), $T_e = 1200$ K.

Thus, the fact that a thin peat bed in the bog does not smolder, as a rule, has been confirmed. This result permits proposing a method for fighting peat fires based on the isolation of smoldering places by pumping water under a small-height reactant layer.

Figure 2 gives the dependence of the ignition time of the reactant on the heat transfer coefficient at $\varphi_{1in} = 0.7$, $\varphi_{2in} = 0.2$, $\rho_{1s} = 750$ kg/m³, $c_{3in} = 0.23$ and the input data from Section 3. From the analysis of the numerical solution of the problem it follows that with increasing intensity of external action (T_e , α_e) the ignition time decreases. As the heat transfer coefficient decreases to $\alpha_e \leq 1.0$ W/(K·m²) for 1000 K $\leq T_e \leq 1100$ K, the smoldering rate does

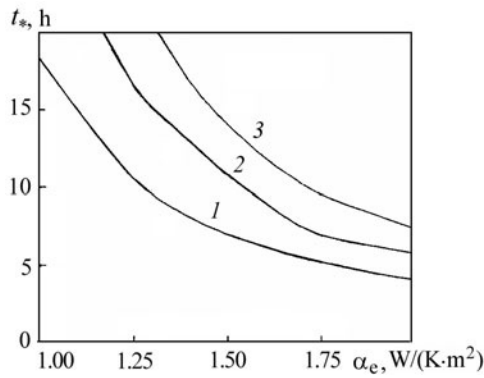


Fig. 2. Ignition time of peat versus the heat transfer coefficient for the external source with a temperature $T_e = 1200$ K (1), 1100 (2), and 1000 (3).

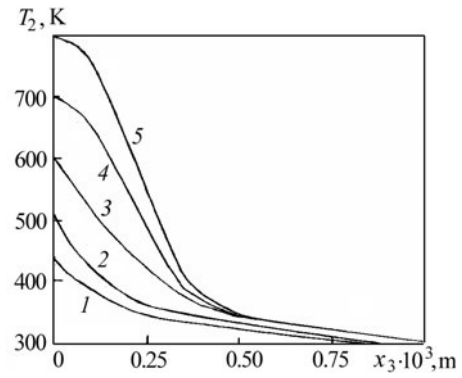


Fig. 3. Temperature distribution of the gas versus the depth of the bed at various instants of time: 1) 4.41 h; 2) 6.41; 3) 8.99; 4) 10.42; 5) 10.83.

not exceed the pyrolysis rate and the sample does not ignite. This is due to both the decrease in the intensity of mass exchange with the environment (insufficient quantity of oxygen in reactant pores) and the increase in the quantity of heat removed into the environment that becomes large and exceeds the quantity of heat supplied by the exothermal oxidation reaction of carbon oxide. A similar effect of the absence of peat smoldering is observed under the conditions of an insignificant initial concentration of oxygen in reactant pores ($c_{3in} < 0.05$) at $T_e \leq 1100$ K and $\alpha_e \leq 1.5$ W/(K·m²).

Figure 3 shows the temperature distribution of the gas phase in the layer depth x_3 at $x_1 = x_2 = c$ (see Fig. 1) at different instants of time for $\varphi_{1in} = 0.7$, $\varphi_{2in} = 0.2$, $c_{3in} = 0.23$, $\rho_{1s} = 750$ kg/m³, $T_e = 1100$ K, $\alpha_e = 1.5$ W/(K·m²) and the input data from Section 3. Note that up to the instant ($t < 10.42$ h) of time of ignition (to the regime of ignition $t = t_*$ there correspond the convex upwards curves in Fig. 3) the temperatures of the gas and the peat framework practically coincide. Then at $t \geq t_*$, as a result of the heat release from the exothermal oxidation reaction of carbon oxide (15) the gas phase temperature T_{2w} exceeds the framework temperature T_{1w} [10].

From the results obtained in [9] and analysis of the numerical solution of the problem, it follows that with increasing temperature of the permeable fragment of the medium, first heating and then evaporation of bound water are observed and, thus, the volume fraction of bound water at $t > 8.99$ h disappears, transforming into the concentration of H₂O vapors [9]. In the high-temperature ($T_1 > 380$ K) region, the process of pyrolysis of the original reactant with the appearance of the great bulk of water vapors and coke begins [9]. Then the pyrolysis product — coke — begins to burn out (smolder) into the depth of the fragment of the porous medium with the formation of ash [9] as a result of the exothermal oxidation reaction.

Figure 4 shows the time dependence of the smoldering rate of peat ω_3 for $0.25 \text{ m} \leq H_i \leq 0.5 \text{ m}$, $i = 1, 2$ from Table 2. The variant $H_1 = 0.5 \text{ m}$ and $H_2 = 0.25 \text{ m}$ at $T_e = 1200$ K for $\alpha_e = 1.75, 1.5,$ and 1.25 W/(K·m²) is marked with numbers 1, 2, and 3, respectively. It is seen that with decreasing mass exchange intensity α_e (of curves 3 and 4, 6 and 7) and temperature of the external combustion site the ignition time of the reactant increases. In so doing, the water layer thickness practically does not influence the ignition time of peat (Table 2). As would be expected, in a thin peat bed with increasing water layer thickness the ignition time of the reactant increases.

It should be noted that the smoldering rate of peat in the near-surface layers $0 \leq x_3 < z_1$ (see Fig. 1) along the sample ω_1 on the left and right of the center of the place of combustion $x_1 = x_2 = c$ is an order of magnitude higher than into the depth ω_3 . This is due to the fact that the spread of smoldering over the near-surface layers proceeds on a preheated porous sample of peat from the side of the surface place of combustion. At the same time the process of smoldering into the depth with the rate ω_3 proceeds in contact with cold underlying layers of the permeable medium. Therefore, one way of fighting peat fires is timely removal of the near-surface layer of smoldering peat.

As a result of the decrease in the oxygen concentration c_{3in} from 0.23 to 0.11 and 0.05, the ignition time of the reactant increases to $t_{*1} = 10.83$ h, $t_{*2} = 11.21$ h, and $t_{*3} = 11.84$ h, which is due to the decrease in the smoldering rate of the reactant as a result of the decrease in the oxidizer content in the peat pores. This result agrees quali-

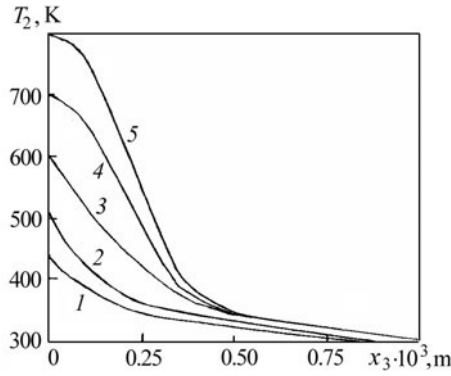


Fig. 4. Time dependence of the linear smoldering rate in the sample depth: 1–3) ($H_1 = 0.5$ m, $H_2 = 0.25$ m, $T_e = 1200$ K, $\alpha_e = 1.75, 1.5, 1.25$ W/(K·m²)); 4–6) obtained at $T_e = 1100$ K and the input data of variants 1–3, 7–8 ($H_2 = 0.5$ m, $T_e = 1000$ K, $\alpha_e = 1.75, 1.5$ W/(K·m²)); 9) ($H_1 = 0.25$ m and 0.25 m $\leq H_2 \leq 0.5$ m (see Table 2)).

tatively with the experimental data of [4] where a method based on the isolation of places of combustion from the ambient air was proposed as a way to fight soil fires.

Of interest is also the investigation of the influence of the content of initial volume fractions of the original reactant and moisture (φ_{in} , $i = 1, 2$) on the smoldering rate of peat. As the volume fraction of moisture decrease from $\varphi_{2in} = 0.1$ to $\varphi_{2in} = 0.05$ for the value of $\varphi_{1in} = 0.7$, there is also a decrease in the ignition time from $t_{*1} = 7.96$ h to $t_{*2} = 6.48$ h. This is mainly due to the decrease in the quantity of heat expended in the evaporation of bound water in peat. As the initial value of the original permeable reactant decreases from $\varphi_{1in} = 0.7$, $\varphi_{1in} = 0.65$ to $\varphi_{1in} = 0.6$ (with increasing initial permeability of peat ξ_{in} : $1 \cdot 10^{-17}$, $3.9 \cdot 10^{-17}$, and $1.04 \cdot 10^{-16}$ m²) for the moisture value $\varphi_{2in} = 0.2$, the ignition time increases: $t_{*3} = 10.83$, $t_{*4} = 11.48$, and $t_{*5} = 11.96$ h, which is due to the increase in the peat porosity — the presence of air that decreases the effective heat conductivity coefficient and increases the heating time of samples. These results agree qualitatively with the experimental data of [11].

CONCLUSIONS

1. We have presented a three-dimensional formulation of the problem on ignition of a peat bed situated over a water stratum taking into account the processes of drying, pyrolysis, and oxidation of gaseous and condensed combustion products and a concrete database.

2. It has been established that as T_e and α_e vary over the ranges 1000 K $\leq T_e \leq 1200$ K and $1.0 \leq \alpha_e \leq 2.0$ W/(K·m²), the time of ignition and smoldering of peat is determined by the intensity of external combustion, the initial oxidizer content in the reactant pores, the drying and pyrolysis process, the exothermal oxidation reaction of carbon oxide, as well as by the height of the peat–water stratum.

3. It has been shown that the results of calculations for the peat moldering rate agree with the experimental data of [2, 4, 11].

4. It has been established that for a high peat bed the ignition time increases with decreasing thickness of the bed while the depth of water under it and the density of the heat flow from the external place of combustion remain unaltered, and for a thin peat layer the ignition time increases with increasing thickness of the water stratum under it.

This work was supported by the Russian Foundation for basic Research (No. 08-01-99019, 11-01-00673-a, 10-01-91054-NTsNI_a).

NOTATION

a_1 , distance from the origin of coordinates on the x_1 axis to the beginning of the place of surface combustion, m; a_2 , distance to the origin of coordinates on the x_2 axis to the beginning of the place of surface combustion, m; A_s , accommodation coefficient; A_v , volume heat transfer coefficient between the gas and condensed phases,

$W/(m^3 \cdot K)$; b_1 , distance from the origin of coordinates on the x_1 axis to the end of the place of surface combustion, m; b_2 , distance from the origin of coordinate on the x_2 axis to the end of the place of ground combustion, m; c_* , distance from the origin of coordinates on x_1, x_2 to the center of the place of surface combustion, m; c_p , heat capacity coefficient, $J/(kg \cdot K)$; c , mass concentration of components; d_p , diameter of cylindrical pores, m; D , diffusion coefficient, m^2/s ; E_i , $i = 1, 2$, activation energy of homogeneous oxidation reactions (15), J/mole; E_{is} , $i = 1, 2, 3$, activation energy of reactions $R_{1s}, R_{2s}, R_{3s}, R_{4s}$ from (7), (16), (17), J/mole; h_{x_i} , $i = 1, 2, 3$, reference steps of the difference scheme on the spatial coordinates, m; H_1, H_2 , thickness of the permeable peat bed and water stratum, m; k , Boltzmann constant, J/K ; k_i , $i = 1, 2$, pre-exponential factors of oxidation reactions, s^{-1} ; k_{is} , $i = \overline{1, 4}$, pre-exponential factors of reactions $R_{1s}, R_{2s}, R_{3s}, R_{4s}$, s^{-1} , $kg/(s \cdot m^2)$, m/s, m/s; L_i , $i = 1, 2, 3$, lengths of the parallelepiped sides in Fig. 1, m; M , molecular weight, $kg/kmole$; P , gas pressure in pores, N/m^2 ; Q , mass rate of formation (disappearance) of the gas phase as a result of homogeneous chemical reactions in peat; q_i , $i = 1, 2$, thermal effects of oxidation reactions (15), J/kg ; q_{is} , $i = \overline{1, 4}$, thermal effects of reactions $R_{1s}, R_{2s}, R_{3s}, R_{4s}$, J/kg ; r_1, r_2 , molar-volume oxidation rates of carbon oxide and methane; R , universal gas constant, $J/(mole \cdot K)$; R_{1s} , mass decomposition rate of dry reactant (peat), $kg/(s \cdot m^3)$; R_{2s} , mass evaporation rate of bound water in peat, $kg/(s \cdot m^3)$; R_{3s} , mass rate of combustion of coke breeze, $kg/(s \cdot m^3)$; R_{4s} , mass rate of formation of ash, $kg/(s \cdot m^3)$; R_α , $\alpha = \overline{1, 5}$, mass rate of formation and disappearance of gas phase components in the diffusion equation (6), $kg/(s \cdot m^3)$; s_2 , specific evaporation surface of water, m^{-1} ; s_3 , specific reaction surface of carbon, m^{-1} ; t , time, h; T_1 , temperature of the peat framework, K; T_2 , temperature of the gas phase in peat pores, K; T , temperature of water under the peat bed, K; T_* , smoldering temperature of peat, K ; \mathbf{W} , speed vector of filtration, m/s; $x_j = c_j M / M_j$, $j = 1, \dots, 5$, molar concentration; $y_i = \rho c_i / M$, $i = 1, 2$, molar-volume concentration, mole/cm³; z_1 , distance from the sample surface to the depth of the porous reactant, m; α , heat transfer coefficient, $W/(K \cdot m^2)$; $\alpha_4 = v_4 M_{4s} / (v_3 M_{3s})$, reduced stoichiometric coefficient [10], and the right-hand side of the third equation of (7) characterizes the mass rate of formation and disappearance of coke breeze; Γ , peat–water conjugate plane; Γ_m , $m = \overline{1, 6}$, faces of the parallelepiped in Fig. 1; β_e , mass transfer coefficient, $kg/(m^2 \cdot s)$; $\epsilon_{j,\alpha}$, potential interaction energy of molecules, J; η_i , $i = \overline{1, 4}$, dimensionless parameters; λ , heat conductivity coefficient, $W/(m \cdot K)$; $\mu = \mu_{in}(T_2/T_{in})^{0.5}$, dynamic viscosity coefficient of the mixture of gases, $kg/(m \cdot s)$; v_3, v_4 , stoichiometric coefficients [10]; $\xi = \xi_* \varphi_5^3 / (1 - \varphi_5)^2$, function describing the influence of the volume fraction of the gas on the resistance; $\xi_* = d_p^2 / 120$, characteristic permeability, m^2 ; ρ , density, kg/m^3 ; ρ_5 , gas phase density, kg/m^3 ; $\sigma_{j,\alpha}$, interaction cross-section of molecules, Å; φ_i , $i = \overline{1, 4}$, dimensionless volume fractions; φ_5 , volume fraction of the gas phase defined by the second formula from (8); ω_3 , linear smoldering rate into the depth of peat at $x_1 = x_2 = c_*$, m/s; ω_1 , linear smoldering rate on the peat surface at $x_3 = 0$, $x_2 = c_*$, m/s. Subscripts: a_i , $i = 1, 2$, lengths given in Fig. 1; w, heated side of the peat surface at $x_3 = 0$; 1, peat framework; 2, gas phase in the porous reactant; s, condensed phase; e, external place of combustion; *, characteristic quantity; c, fraction of coke in the course of the pyrolysis reaction of peat; in, initial value; $\alpha = 1, \dots, 6$, correspond in the gas phase to carbon oxide, water vapors, carbon dioxide, methane, and nitrogen; 1s, ..., 4s, in the condensed phase — peat, bound water, coke, ash; p, pore; v, volume.

REFERENCES

1. A. M. Grishin, *Mathematical Models of Forest Fires* [in Russian], Izd. Tomsk Univ., Tomsk (1981).
2. A. A. Borisov, Al. A. Borisov, R. S. Gorelik, et al., Experimental investigation and mathematical modeling of peat fires, in: *Thermal of Forest Fires* [in Russian], Izd. Inst. Teplofiz. SO AN SSSR, Novosibirsk (1984), pp. 5–22.
3. A. A. Borisov, Ya. S. Kisilev, and V. P. Udilov, Kinetic characteristics of the low-temperature combustion of peat, in: *Thermophysics of Forest Fires* [in Russian], Izd. Inst. Teplofiz. SO AN SSSR, Novosibirsk (1984), pp. 23–30.
4. S. V. Gundar, Determination of the minimum concentration of oxygen in flameless combustion of soil, *Lesnoe Khoz.*, No. 5, 53–54 (1976).
5. A. N. Subbotin, Mathematical modeling of the propagation of the fire front in peat bogs, in: *Mechanics of Reacting Media and Its Applications* [in Russian], Nauka, Novosibirsk (1989), pp. 57–63.
6. A. N. Subbotin, On the features of the underground fire propagation, *Inzh.-Fiz. Zh.*, **76**, No. 5, 159–165 (2003).

7. A. M. Grishin, General mathematical models of forest and peat fires and their applications, *Usp. Mekh.*, **1**, No. 4, 41–89 (2002).
8. A. M. Grishin, A. S. Yakimov, G. Rein, and A. Simeoni, On physical and mathematical modeling of the initiation and propagation of peat fires, *Inzh.-Fiz. Zh.*, **82**, No. 6, 1210–1217 (2009).
9. A. M. Grishin and A. S. Yakimov, Mathematical modeling of the process of peat ignition, *Inzh.-Fiz. Zh.*, **81**, No. 1, 191–199 (2008).
10. A. M. Grishin and A. S. Yakimov, Mathematical modeling of the thermophysical processes in peat ignition and smoldering, *Teplofiz. Aeromekh.*, **17**, No. 1, 151–167 (2010).
11. A. M. Grishin, A. N. Golovanov, Ya. V. Sukov, and Yu. I. Preis, Experimental study of the ignition and combustion peat, *Inzh.-Fiz. Zh.*, **79**, No. 3, 137–142 (2006).
12. A. M. Grishin, A. N. Golovanov, and Ya. V. Sukov, Experimental determination of the thermophysical, thermokinetic, and filtration characteristics of peat, *Inzh.-Fiz. Zh.*, **79**, No. 3, 131–136 (2006).
13. A. M. Grishin, A. N. Golovanov, and A. S. Yakimov, Conjugate heat transfer in a composite material, *Prikl. Mekh. Tekh. Fiz.*, No. 4, 141–148 (1991).
14. A. M. Grishin and V. M. Fomin, *Conjugate and Nonstationary Problems of the Mechanics of Reacting Media* [in Russian], Nauka, Novosibirsk (1984).
15. B. V. Alekseev and A. M. Grishin, *Physical Gas Dynamics of Reacting Media* [in Russian], Vysshaya Shkola, Moscow (1985).
16. E. S. Shchetinkov, *Physics of the Combustion of Gases* [in Russian], Nauka, Moscow (1965).
17. E. C. Campbell and R. M. Fristrom, Reaction kinetics, thermodynamics, and transport in the hydrogen bromine system, *Chem. Rev.*, **38**, No. 2, 173–234 (1958).
18. V. V. Pomerantsev (Ed.), *Principles of the Practical Theory of Combustion* [in Russian], Énergiya, Leningrad (1973).
19. K. P. Mishchenko and A. A. Ravdel', *Concise Handbook of Physicochemical Quantities* [in Russian], Khimiya, Leningrad (1972).
20. A. M. Grishin, V. I. Zinchenko, K. N. Efimov, A. N. Subbotin, and A. S. Yakimov, *Iteration-Interpolation Method and Its Applications* [in Russian], Izd. Tomsk Univ., Tomsk (2004).
21. A. V. Lazarev and S. S. Korchunov (Eds.), *Handbook on Peat* [in Russian], Nedra, Moscow (1982).
22. M. P. Vukalovich, S. A. Rivkin, and A. A. Aleksandrov, *Tables of the Thermal Properties of Water and Steam* [in Russian], Izd. Standartov, Moscow (1969).